Electrocatalytic reduction of CO2 and nitrate on immobilized metal porphyrins

Shen, Jing

Chapter 3

DFT Study on the Mechanism of the Electrochemical Reduction of CO_2 Catalyzed by Cobalt Porphyrin

ABSTRACT

The electrochemical reduction of CO_2 is a promising way to store renewable energy in fuels or other chemicals. However, the high overpotential and low efficiency of the reaction hinder the development of the area. More work is needed on the investigation of the mechanism in order to obtain new insights into developing effective catalysts. We report here a density functional theory (DFT) study of the electrochemical reduction of CO_2 on a cobalt porphyrin. The CO_2^- anion adduct is demonstrated to be the key intermediate formed only when the cobalt center of the complex is in the Co^I oxidation state. We find that formic acid can be produced as minor product through $[Co(P)\text{-}(OCHO)]^-$ as intermediate, while CO is the main product through a decoupled electron-proton transfer. CH_4 is produced as minor product from subsequent CO reduction by concerted proton-coupled electron transfer assumed at each electrochemical step. Our theoretical interpretations are consistent with the experimental results presented in Chapter 2, and give deeper insights into the mechanism of the CO_2 electrochemical reduction on cobalt porphyrin complexes.

This chapter has been submitted as: Jing Shen, Manuel J. Kolb, Adrien J. Göttle and Marc T.M. Koper. *J. Phys. Chem.C*.

3.1. Introduction

In nature, carbohydrates are produced from CO_2 from the atmosphere by utilizing sun light through photosynthesis. The fossil energy crisis and current excess emissions of CO_2 urgently call for a new utilization of CO_2. Mimicking natural photosynthesis, the electrochemical reduction of CO_2 is a promising method to store renewable energy such as sunlight and wind into small organic molecules. Different kinds of products can be produced, such as carbon monoxide (CO), formic acid (HCOOH), formaldehyde (HCHO), methanol (CH_3OH), methane (CH_4) and even ethylene (C_2H_4) in aqueous solution[1-4], or oxalate ($C_2O_4^{2-}$) mainly in aprotic solvents. However, there are still challenges in the electrochemical reduction of CO_2. One important challenge is that the reaction requires considerable overpotentials, especially those reactions yielding products that need the transfer of more than 2 electron[5]. The other challenge is that the hydrogen evolution reaction is a competing reaction with CO_2 reduction, which often leads to hydrogen as dominant product (as hydrogen is a 2-electron product).

Different kinds of catalysts have been utilized for the the electrochemical eduction of CO_2 in order to reduce the reaction overpotential. Hori et al. have made a comprehensive investigation on different metal catalysts which give different products depending on the nature of the metal and the experimental conditions[6]. Copper, for which a reasonable understanding of the mechanism has been obtained, is an exceptional catalyst which gives CH_4, C_2H_4 and ethanol (CH_3CH_2OH) as main products[7-9]. Metal complexes, especially with phthalocyanine, porphyrin and cyclam ligands[10-12], have also been used as catalysts for the electrochemical reduction of CO_2 and mainly lead to 2-electron transfer products, such as CO, HCOOH and $C_2O_4^{2-}$ (in aprotic solvents). The speculation on the first intermediate is that it is either a $CO_2^{\bullet-}$ anion radical which gains a proton or a CO_2 that inserts into metal hydride to form –OCHO[9]. Tripkovic et al.[13] have performed first-principles density functional theory calculations on the possible product spectrum of the electrochemical reduction of CO_2 and CO on metal-functionalized porphyrin-like graphene surfaces. HCOOH was found by them as an end product wherea CO is a precursor for more reduced products like methanol and methane. They claim that M-COOH is the key intermediate for

further reaction, which is competing with M-H. Nielsen and Leung et al.[14,15] have investigated in detail the formation of CO on a Co-based porphyrin. Their mechanism involves the $[Co(P)-(CO_2)]^{2-}$ intermediate which is subsequently protonated to give $[Co(P)-(COOH)]^-$. The latter species readily decomposes to give CO. In Chapter 2 we studied the pH dependence of the electrochemical reduction of CO_2 on a cobalt protoporphyrin immobilized on a pyrolytic graphite electrode[16]. From our results, we proposed a mechanism in which a CO_2^- anion adduct forms first. The CO_2^- anion adduct will subsequently be protonated by a water molecule to give the $[Co(P)-(COOH)]^0$ intermediate. The $[Co(P)-(CO)]^0$ intermediate which is formed next will either form CO as a product or be further reduced to CH_4 through a series of concerted proton-electron transfer reactions.

In this Chapter, we report on a theoretical study using DFT calculations of the electrochemical reduction of CO_2 on cobalt porphyrin complex (the simplest porphyrin ligand) in aqueous solution. Our calculations emphasize the anionic character of the CO_2 when bound to the reduced $[Co^IP]^-$ complex. This is due to the charge transfer from the metal center to the substrate upon binding. The formation of CO takes place through the $[Co(P)-(COOH)]^0$ intermediate. The [Co(P)-(OCHO)] intermediate, which gives formic acid as minor product, competes with the formation of the [Co(P)-(COOH)] intermediate. The formation of CH_4 and CH_3OH is studied assuming concerted proton-electron transfer steps.

3.2. Computational Method

DFT calculations have been performed with the Amsterdam Density Functional program (ADF 2014.06)[17]. The revised version of Perdew-Burke-Ernzerhof exchange-correlation functional RPBE[18] was used together with Grimme's dispersion correction D3[19]. For all atoms, a Slater type basis set of triple-ζ quality including a polarization function has been used (TZP)[20]. Geometries have been fully optimized with the conductor-like screening model (COSMO)[21-23] to account for solvation effects (water). We have considered both the low spin and high spin electronic configurations for each geometry. In all cases, the energy of the low spin configuration is the lowest except for the $[Co(P)-(OCHO)]^-$ intermediate. The $[Co(P)-(CH_2)]^-$ intermediate is only stable at high spin state (shown in Appendix B

Table 1). Frequency calculations have been performed to check that the optimized geometries are actual minima on the potential energy surface and also to obtain Gibbs free energies. Since the analytical frequencies are not available in ADF when using D3 dispersion corrections, we used the finite temperature and entropic contributions computed from geometries optimized at the RPBE/TZP/COSMO calculation level and added these contributions to the energy computed with RPBE-D3. The standard equilibrium potentials of electrochemical steps were computing using the computational hydrogen electrode (CHE) model[24]. This model allows treating electrochemical reactions as if they were chemical by making use of the definition of the standard hydrogen electrode. However, the CHE model is restricted to steps in which an equal number of protons and electrons are transferred (concerted proton-electron transfer). The values of the corresponding potentials for concerted proton-electron transferred reactions are calculated as:

$$E^0 = -\Delta G/e$$

Where ΔG is the free energy change of the reaction, e is the elementary charge, and E^0 is the standard equilibrium potential.

3.3. Results and Discussion

3.3.1. Activation of CO_2 to CO and HCOOH

In our recent work[16], we found that the onset potential of both the CO_2 reduction and hydrogen evolution reaction (-0.5 V) is very close to the redox potential of the $Co^{II}P/Co^{I}P$ couple (-0.6 V)[25]. This strongly indicates that the catalytic reaction is triggered by the initial reduction of the catalyst. We also concluded that CO_2 is activated by its association with the reduced catalyst $[Co^{I}P]^-$. Based on literature and their own DFT calculations, Nielsen and Leung et al. have also concluded that CO_2 binds to the Co^{I} oxidation state of the porphyrin[14-15]. In the adduct $[Co(P)-(CO_2)]^-$ that is formed, we assumed that CO_2 is bound as a CO_2^- anion which explains the basicity of this species. Therefore, in the mechanism we proposed from the experiment, the first electro-proton pair addition goes through a

decoupled electron transfer-proton transfer (ET-PT) mechanism. The corresponding sequence of reactions proposed is therefore:

$$[CoP]^0 + e^- \longrightarrow [CoP]^- \quad (1)$$

$$[CoP]^- + CO_2 \longrightarrow [Co(P)\text{-}(CO_2)]^- \quad (2)$$

We have investigated the basic character of the $[Co(P)\text{-}(CO_2)]^0$ and $[Co(P)\text{-}(CO_2)]^-$ adduct as they are the key point to explain the pH dependence of the CO_2 reduction observed experimentally. To do so, we have performed a Mulliken charge analysis of $[CoP]^0$ and $[CoP]^-$ intermediates to know where the additional charge is localized after reduction of the catalyst (eq. 1), and of the $[CoP\text{-}CO_2]^-$ adduct to address how the charge is redistributed upon the binding of CO_2 to the reduced catalyst (eq. 2). Both $[CoP]^0$ and $[CoP]^-$ complexes have a planar structure. The Co-N distance in $[CoP]^-$ is 1.976 Å which is slightly shorter than in $[CoP]^0$, which is 1.994 Å. The Mulliken charge on cobalt center is +0.87 for $[CoP]^0$ and +0.47 for $[CoP]^-$, respectively, while the charges on nitrogen atoms are -0.52 for both molecules. Therefore, in the negatively charged porphyrin, a significant amount of the extra negative charge is located on cobalt atom. We have tried to optimize CO_2 adduct with both the neutral and negatively charged complex. Any attempt to optimize CO_2 adduct with the neutral complex failed, which indicates that the neutral CO_2 adduct is not stable (no minimum on the potential energy surface). By contrast, we managed to optimize the negatively charged CO_2 adduct, $[Co(P)\text{-}(CO_2)]^-$. It is important to note that the negatively charged CO_2 adduct is not stable without solvation. This can be explained by the fact that a significant charge transfer from the cobalt atom to the CO_2 adduct occurs upon the binding process, and the presence of a polar solvent is crucial to stabilize this charge transfer process. However, the binding process is almost thermoneutral (see Table 1). The structure of $[Co(P)\text{-}(CO_2)]^-$ complex is shown in Figure 1(a) and some relevant parameters have been collected in Table 1. In the $[Co(P)\text{-}(CO_2)]^-$ molecule, the distances of Co-N bonds are 1.991 Å which are elongated compared to the bare $[CoP]^-$ molecule. This may indirectly indicate that the electronic state of cobalt center has been changed upon CO_2 binding, back to the length of the Co-N bonds corresponding to the neutral $[CoP]^0$ complex

with Co^{II} oxidation state. The bond angle of O-C-O of adsorbed CO_2 is 134° . Compared to the bond angle of O-C-O of the CO_2 gas-phase molecule (180°), adsorbed CO_2 is bent. The calculated bond angle of O-C-O for CO_2^- in the gas phase is 133.2°. The Mulliken charge analysis for $[Co(P)-(CO_2)]^-$ and gas-phase CO_2 molecule shows that the charge on the cobalt atom in $[Co(P)-(CO_2)]^-$ molecule is +0.62, and the total charge on CO_2 molecule is -0.61 with +0.56 on the C atom and -0.59 on the two O atoms. Compared to the charge centered on cobalt atom of $[CoP]^-$ (+0.47) and on the carbon and oxygen atoms of gas CO_2 molecule, +0.87 and -0.44, respectively, we conclude that there is partial charge transfer from cobalt atom to CO_2 in $[Co(P)-(CO_2)]^-$ complex. In order to understand the origin of this charge transfer, we have analyzed the interaction between the cobalt and CO_2 using the molecular orbitals. Figure 1b shows the space representation of the HOMO-2 orbital which is responsible for most of the interaction between the cobalt and CO_2 in the $[Co(P)-(CO_2)]^-$ molecule. In Appendix B Figure 2, we also show the space representations of the first four highest occupied molecular orbitals (HOMO to HOMO-3). From Appendix B Figure 2 we can see that HOMO and HOMO-1 orbitals show no interaction between cobalt atom and CO_2 adduct, while HOMO-2 and HOMO-3 orbitals contribute to the interaction with different orientation. Therefore, we mainly focus on the HOMO-2 orbital to obtain an insight into the charge transfer. From Figure 1b we see that this orbital consists of the mixing of a hybrid metallic orbital (d_z^2 (ca. 20%) and d_x^2-$_y^2$ (ca. 40%)) with the antibonding π* orbital (ca. 40%) of CO_2. Therefore, the orbital interaction between the Co *d* state and the CO_2 π* orbital leads to a net charge delocalization from the cobalt to the CO_2. A similar conclusion was reached by Meshitsuka et al.[26] who suggested that the occupied d_z^2 orbital of the metal atom of a phthalocyaline complex plays an important role in the activation of CO_2.

To unravel the details of the mechanism of the CO_2 reduction to CO, we have first computed the equilibrium potential of the reaction step where the binding of the substrate and both the proton and electron addition are concerted (shown in Table 2).

$$[CoP]^0 + CO_2 + H^+ + e^- \longrightarrow [CoP\text{-}COOH]^0 \qquad (3)$$

Table 1: Binding of CO_2 to $[CoP]^-$ including solvation.

ΔG/ eV	q_{CO2} *	q_{Co} *	∠OCO /° *	r_{Co-N} /Å *
0.09	-0.61 (0)	0.62 (0.47)	134 (180)	1.991 (1.976)

* The numbers in the brackets correspond to the value of the CO_2 gas molecule and $[CoP]^-$ in their non-bonded state.

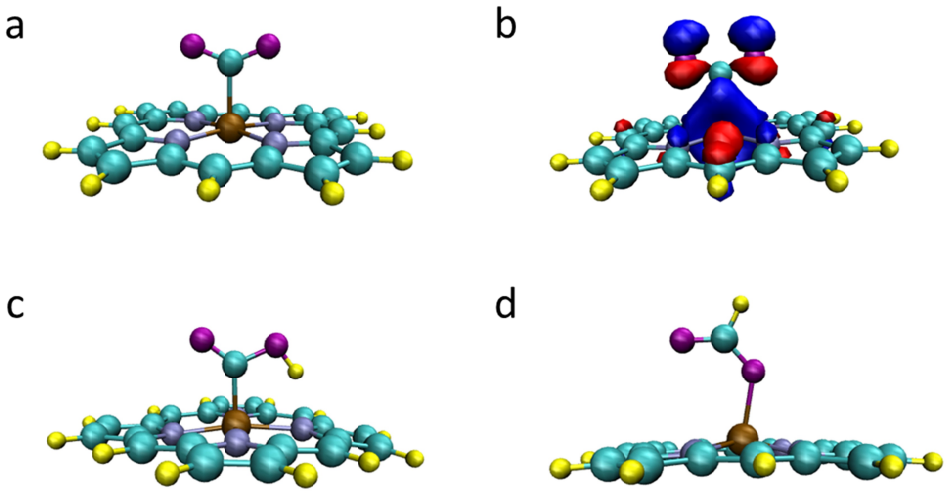

Figure 1 Optimized geometries of intermediates: (a) CO_2^- anion adduct on $[CoP]^-$, i.e. $[Co(P)\text{-}(CO_2)]^-$; (b) spatial representation of HOMO orbital of $[Co(P)\text{-}(CO_2)]^-$; (c) negatively-charged $[Co(P)\text{-}(COOH)]^-$ intermediate; (d) negatively charged $[Co(P)\text{-}(OCHO)]^-$ intermediate.

The computed equilibrium potential of this reaction (-0.43 V, shown in Table 2) is similar to the onset potential found experimentally (-0.5V). Therefore, we will refer to this potential as E_{onset}. This indicates that the concerted pathway can proceed, based on its thermodynamics, for E_{onset} and more negative potentials. As mentioned, any attempts to try to optimize the neutral $[Co(P)\text{-}(CO_2)]^0$ adduct invariably resulted in the dissociation of CO_2 from the complex. In contrast, we managed to optimize the anionic $[Co(P)\text{-}(CO_2)]^-$ adduct.

Furthermore, we have checked how the energy of the neutral and anionic complexes [Co(P)-(CO_2)] varies as the CO_2 approaches the metallic center at large Co-$C_{(CO2)}$ distances (shown in Appendix B Figure 1). To do so, we have created constrained structures corresponding to the optimized structure of the [Co(P)-(CO_2)]$^-$ adduct for which the Co-$C_{(CO2)}$ distance is elongated by 1 Å and decreased step by step the Co-$C_{(CO2)}$ distance to its initial value while all other parameters were fully relaxed at each step (relaxed scan). The corresponding energy profiles are reported in Appendix B (Figure 1). For the anionic complex, the energy continues to decrease as the CO_2 approaches the cobalt. The binding of CO_2 to the reduced catalyst (eq. 2) is therefore a barrierless process. In contrast, the energy increases for the neutral complex following the same reaction coordinate ($\Delta E \sim 0.7$ eV when Co-C distance is elongated by 0.5 Å from its optimized value in [Co(P)-(CO_2)]$^-$). This suggests that for the neutral complex the activation energy for the concerted pathway is large as the transition state of this step necessarily requires the approach between CO_2 and the catalyst. As a result, although the concerted pathway is possible based on its thermodynamics when $E_{applied} \leqslant -0.43$ V, it is kinetically slow or even hindered at room temperature due to a large thermal activation barrier. In contrast, as the association of CO_2 with the reduced catalyst has no thermal activation barrier (though we emphasize that this "barrier" is not a free energy barrier since no entropy corrections were included), the formation of the [Co(P)-(CO_2)]$^-$ adduct can readily proceed whenever the applied potential is suitable. The conclusion from our calculations is in agreement with what we proposed from the experimental results with the formation of the [Co(P)-(CO_2)]$^-$ intermediate.

Table 2: Computed equilibrium potentials for indicated reactions.

	Reaction Equation	E^0 /V_{RHE} With solvation
Reaction (3)	$[CoP]^0 + CO_2 + H^+ + e^- \longrightarrow [Co(P)\text{-}(COOH)]^0$	-0.43
Reaction (5)	$[Co(P)\text{-}(CO_2)]^- + H^+ + e^- \longrightarrow [Co(P)\text{-}(COOH)]^-$	-1.01
Reaction (6)	$[Co(P)\text{-}(COOH)]^0 + H^+ + e^- \longrightarrow [Co(P)\text{-}(CO)]^0 + H_2O$	0.16
Reaction (7)	$[Co(P)]^0 + CO_2 + H^+ + e^- \longrightarrow [Co(P)\text{-}(OCHO)]^0$	-0.92
Reaction (8)	$[Co(P)\text{-}(CO_2)]^- + H^+ + e^- \longrightarrow [Co(P)\text{-}(OCHO)]^-$	-0.21
Reaction (10)	$[Co(P)\text{-}(OCHO)]^- + H^+ + e^- \longrightarrow [CoP]^- + HCOOH$	-0.07
Reaction (11)	$[Co(P)\text{-}(OCHO)]^- + H^+ + e^- \longrightarrow [Co(P)\text{-}(OCH_2O)]^-$	-1.79
Reaction (12)	$[CoP]^0 + H^+ + e^- \longrightarrow [Co(P)\text{-}(H)]^0$	-0.23
Reaction (13)	$[CoP]^- + H^+ + e^- \longrightarrow [Co(P)\text{-}(H)]^-$	-0.10

After the formation of [Co(P)-(CO2)]-, the next step can be either the protonation or the hydrogenation of this reaction intermediate:

$$[Co(P)\text{-}(CO_2)]^- + H^+ \longrightarrow [Co(P)\text{-}(COOH)]^0 \quad (4)$$

$$[Co(P)\text{-}(CO_2)]^- + H^+ + e^- \longrightarrow [Co(P)\text{-}(COOH)]^- \quad (5)$$

The structure of the $[Co(P)\text{-}(COOH)]^-$ intermediate is displayed in Figure 1c. $[Co(P)\text{-}(COOH)]^0$ has a similar structure as the negatively charged complex. The latter has a shorter $Co\text{-}C_{(COOH)}$ bond length than the former which indicates a stronger interaction between the cobalt atom and the $C_{(COOH)}$ in $[Co(P)\text{-}(COOH)]^-$. Reaction step (5) has a relatively negative equilibrium potential (-1.01 V, see in Table 2), much more negative than the onset potential (-0.5 V). Therefore, the formation of the $[Co(P)\text{-}(COOH)]^-$ intermediate is unlikely if the applied potential is close to the onset potential. Therefore, after formation of $[Co(P)\text{-}(CO_2)]^-$, reaction (4) is likely to occur to form the neutral $[Co(P)\text{-}(COOH)]^0$

intermediate. The sequence of reactions predicted by our calculations (1), (2) and (4) matches the decoupled ET-PT mechanism we proposed from the experimental results[16].

After the formation of the $[Co(P)\text{-}(COOH)]^0$ intermediate, it can be subsequently undergo the following concerted electron-proton transfer step:

$$[Co(P)\text{-}(COOH)]^0 + H^+ + e^- \longrightarrow [Co(P)\text{-}(CO)]^0 + H_2O \quad (6)$$

The equilibrium potential of this reaction step is 0.16 V which indicates that it should spontaneously occur at applied potentials $E \leqslant E_{onset}$. The $[Co(P)\text{-}(CO)]^0$ intermediate can either desorb CO (the binding energy of CO is -0.26 eV) or the bound CO can be further reduced to CH_4 (see below).

Apart from the formation of the ''carboxyhydroxyl" $[Co(P)\text{-}(COOH)]^0$ and $[Co(P)\text{-}(COOH)]^-$ intermediates, "formate-type" intermediates $[Co(P)\text{-}(OCHO)]^0$ and $[Co(P)\text{-}(OCHO)]^-$ (the structure of $[Co(P)\text{-}(OCHO)]^-$ is shown in Figure 1d) can be produced through alternative competing reaction pathways. We assume this "formate-type" intermediate can be produced through the following reaction steps:

$$[CoP]^0 + CO_2 + H^+ + e^- \longrightarrow [Co(P)\text{-}(OCHO)]^0 \quad (7)$$

$$[CoP\text{-}CO_2]^- + H^+ + e^- \longrightarrow [Co(P)\text{-}(OCHO)]^- \quad (8)$$

Like reaction (3), reaction step (7) is associated with the concerted substrate binding and electron-proton transfer. Its equilibrium potential is significantly negative (-0.92 V). In contrast, the equilibrium potential of reaction (8) is much less negative (-0.21 V). It is noteworthy that any attempts to optimize, from a premade structure, a [Co(P)-(OCHO)] adduct where the CO_2 is bonded by one oxygen to the Co center, failed and invariably resulted in the dissociation of the CO_2 for both neutral and anionic charge state. Like for the formation of $[Co(P)\text{-}(COOH)]^0$ through the fully concerted pathway (reaction (3)), reaction (8) is probably kinetically hindered by a large thermal activation barrier due to the switching of the binding mode of the CO_2 from C-bonded to O-bonded to form [Co(P)-

$(OCHO)]^-$. After the formation of $[Co(P)-(OCHO)]^-$, the next possible steps can be either the protonation (reaction (9)) or the concerted electron-proton transfer (reaction (10)) to form formic acid as final product:

$$[Co(P)-(OCHO)]^- + H^+ \longrightarrow [CoP]_0 + HCOOH \quad (9)$$

$$[Co(P)-(OCHO)]^- + H^+ + e^- \longrightarrow [CoP]^- + HCOOH \quad (10)$$

Or, if no desorption occurs, the concerted electron-proton transfer can form the intermediate $[Co(P)-(OCH_2O)]^-$:

$$[Co(P)-(OCHO)]^- + H^+ + e^- \longrightarrow [Co(P)-(OCH_2O)]^- \quad (11)$$

The equilibrium potential of reaction (11) is -1.79 V which is much more negative than the experimental onset potential. This indicates that this reaction is unlikely to occur in the potential range we investigated (0 V~-1.5 V). This is consistent with the results obtained for the electrochemical reduction of formic acid by combining on-line electrochemical mass spectroscopy (OLEMS) and cyclic voltammetry (CV) which show that this species cannot be further reduced and is thus an end product.

CO_2 could also insert into metal hydride to form the [Co(P)-(OCHO)] intermediate. The formation of the neutral and negatively charged metal hydride is through the following reactions:

$$[CoP]^0 + H^+ + e^- \longrightarrow [Co(P)-(H)]^0 \quad (12)$$

$$[CoP]^- + H^+ + e^- \longrightarrow [Co(P)-(H)]^- \quad (13)$$

As shown in Table 2, the equilibrium potentials for reaction (12) and (13) are -0.23 V and -0.10 V, respectively. This indicates that metal hydride is thermodynamically easy to form at E_{onset}. After the formation of metal hydride, H_2 could be produced spontaneously through a concerted proton-electron transfer process with the equilibrium potential of 0.23 V and 0.10 V for the neutral and negatively charged metal hydride, respectively.

Simultaneously, CO_2 could insert into metal hydride as a competing reaction through a chemical step; the free energies (ΔG) for the formation of the $[Co(P)-(OCHO)]^0$ and $[Co(P)-(OCHO)]^-$ intermediate from the final states ort reaction (12) and (13) are 0.69 eV and 0.20 eV, respectively.

Finally, as far as the competition between the formation of CO and formic acid is concerned, when the applied potential is close to the onset potential the selectivity between the two products is governed by the relative efficiencies of the reaction pathways that leads to their formation: the sequence of reactions (1), (2), (8) and (9) or (10) for formic acid formation and sequence of reactions (1), (2), (4) and (6) for CO formation. Since reaction (8) is presumably kinetically slow due to the switching of the CO_2 binding mode, the formation of formic acid is less competitive than the formation of CO. This is consistent with our experimental work in which we found that formic acid is produced as a minor product.

3.3.2. Reduction of CO to CH_4

In the previous section, we studied the formation of [Co(P)-(COOH)] which will form the [Co(P)-(CO)] as the next intermediate. This weakly bonded CO can either be released from complex to form the main product CO or be further reduced to produce CH_4 as minor final product. We speculate that the formation of CH_4 involves concerted proton-coupled electron transfer at each step. Therefore, pathways for CH_4 formation have been calculated using the CHE model. Figure 2 shows the most favorable pathway at two different potentials. The intermediate [Co(P)-(CO)] is first hydrogenated by proton-electron transfer to form [Co(P)-(CHO)], which will be further hydrogenated to form $[Co(P)-(OCH_2)]$. Experimentally, we confirmed that formaldehyde is probably an intermediate for CH_4 formation as the electrochemical reduction of formaldehyde and CO_2 under same conditions both give methane[16]. $[Co(P)-(OCH_2)]$ is subsequently hydrogenated to form the $[Co(P)-(OCH_3)]$ intermediate. Thermodynamically $[Co(P)-(OCH_3)]$ prefers to form methanol as product as compared to [Co(P)-(O)] and CH_4 as Tripkovic et al. have shown previously[13]. In our experiments, no significant amount of methanol was detected. In order

to make sure if methanol could be an intermediate for CH_4 formation from the CO_2 electrochemical reduction, the electrochemical reduction of methanol was studied under the same conditions as CO_2 reduction in Chapter 2[16] by combining CV (Cyclic Voltammetry) with OLEMS. The result is shown in Figure 3, showing that hydrogen is the main product but with CH_4 as minor by-product, which must be the result of methanol reduction. Therefore, we conclude that at sufficiently negative potential methanol may be reduced to CH_4. According to our DFT calculations, application of a potential of -0.51 V (vs RHE) makes the whole pathway from CO_2 to methane downhill, as shown by the brown line in Figure 2. This applied potential of -0.51 V is the onset potential for the potential-determining step in the mechanism, which agrees quite well with the onset potential we observe in experiment. At this potential, [Co(P)-(O)] is unstable and methanol will be reduced to methane.

Competing pathways have also been calculated, as shown in Figure 2, in addition to the most favorable pathway. The formation of [Co(P)-(COH)] is a competing reaction with [Co(P)-(CHO)] formation. The free energy change calculated for [Co(P)-(COH)] formation is 2.34 eV (with a corresponding potential of -2.34 V), which indicates that [Co(P)-(COH)] formation is thermodynamically unfavorable. [Co(P)-(CH_2O)] is a competing intermediate with [Co(P)-OCH_2]. The free energy difference for the reaction from [Co(P)-(CHO)] to [Co(P)-(CH_2O)] is -0.45 eV indicating a thermodynamically favorable reaction. The subsequent protonation of [Co(P)-(CH_2O)] will sequentially form the [Co(P)-(CH_2OH)] and [Co(P)-(CH_2)] intermediates. The free energy changes for these two reactions are 0.77 eV and 0.81 eV, respectively. The high free energy changes for both intermediates indicate that the further reduction of [Co(P)-(CH_2O)] is not thermodynamically favorable. Therefore we consider [Co(P)-(CH_2O)] an unlikely intermediate in a pathway toward methane formation, though ultimately the calculation of the free energy barrier will be necessary to determine which intermediate leads to [Co(P)-(OCH_3)] and finally to methane. Both [Co(P)-(OCH_2)] and [Co(P)-(CH_2O)] may dissociate from the complex to form formaldehyde. The free energy changes for those two processes are -0.93 eV and -0.03 eV, respectively. Note that, in the CHE method, application of a potential U pulls down the free energy change of each electrochemical step by eU eV, but has no effect on the energetics of a chemical reaction.

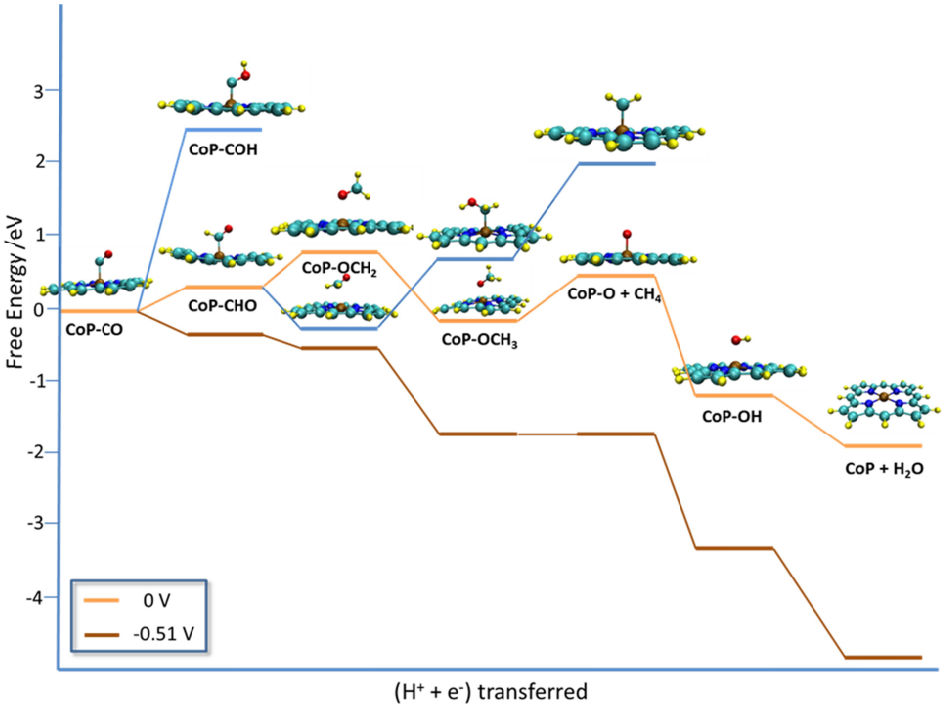

Figure 2 The possible pathways for CH_4 formation from [Co(P)-(CO)]. The Figure shows the most favorable pathway with applied potential U = 0 V (orange line), and the most favorable pathway with applied potential U = -0.51 V (brown lines), which makes each step downhill. Competing pathways are showing in blue lines.

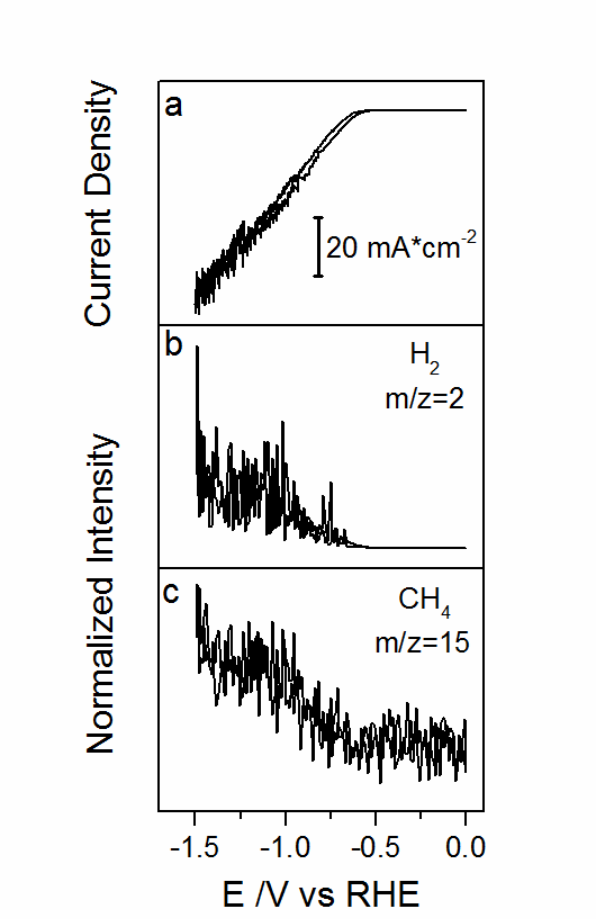

Figure 3 OLEMS measurements of the electrochemical reduction of methanol in 0.1 M $HClO_4$ solution with cyclic voltammetry, the concentration of methanol is 0.05 mol/L. (a) Cyclic Voltammetry, scan rate: 1 mV s^{-1}; (b) H_2 formation measured using OLMES, m/z=2; (c) CH_4 formation measured using OLEMS, m/z=15, the signal is not corrected from methanol. The OLEMS signal has been normalized by dividing the signal with the highest ion current. All experimental conditions as in ref[16].

3.4. Conclusions

In Chapter 2, we concluded that during electrocatalytic CO_2 reduction a CO_2^- anion bound to a Co-porphyrin is produced and acts as a Brønsted-base abstracting a proton from a nearby water molecule to form the [Co(P)-(COOH)] intermediate. Our DFT calculations presented here show that the Co^I oxidation state is the catalytically active state for [Co(P)-(CO_2)]$^-$ formation, in agreement with previous work by Nielsen and Leung[14-15], and consistent with our conclusions from the experiments. In the [Co(P)-(CO_2)]$^-$ complex, there is effective electron transfer from the Co atom to the CO_2 through the interaction between the hybrid $d_{x^2-y^2}$ and d_{z^2} orbital of the Co and the π^* antibonding orbital of the CO_2 such that the CO_2 resembles a CO_2^- anion and Co regains some of its Co^{II} character. Proper solvation correction appears to be very important for obtaining reliable energetics, underscoring the charge transfer character of the complex.

The formation of the [Co(P)-(COOH)]^n (n=0 or -1) intermediate through the concerted electron-proton transfer step is not favorable. The equilibrium potential of the formation of [Co(P)-(COOH)]^0 is slightly less negative than the experimental onset potential. However, CO_2 does not adsorb on the [CoP]^0 intermediate. The formation of [Co(P)-(COOH)]$^-$ has a large negative equilibrium potential, which makes it is thermodynamically unfavorable. Therefore, the formation of the [Co(P)-(COOH)]^n (n=0 or -1) goes through a decoupled electron-proton transfer process, with [Co(P)-(CO_2)]$^-$ as an intermediate. The [Co(P)-(COOH)]^0 intermediate reacts with a further electron and proton to produce [Co(P)-(CO)], which subsequently leads to either the formation of CO or to the transfer of more electrons and protons to produce the 8-electron transfer product CH_4.

The formation of the [Co(P)-(OCHO)] intermediate undergoing a concerted electron-proton transfer step is a competing reaction with the formation of the [Co(P)-(COOH)] intermediate. The formation of [Co(P)-(OCHO)]^0 is thermodynamically difficult as the equilibrium potential of the reaction is significantly negative (-0.92V). In contrast, the equilibrium potential of the formation of the [Co(P)-(OCHO)]$^-$ intermediate is less negative than experimental onset potential. However, it is probably kinetically slow as the

binding atom of CO_2 changed from C-bounded to O-bounded. The formic acid can be produced from the hydrogenation or protonation of the [Co(P)-(OCHO)] intermediate. Therefore, the formic acid is a minor product compare to the CO. The further reduction of [Co(P)-(OCHO)] is difficult because of the negative equilibrium potential for the formation of $[Co(P)-(OCH2O)]^-$, -1.79 V. From our experiments, we indeed found only a minor amount of formic acid formation and that the formic acid was not further reduced.

The formation of CH_4 from CO reduction was studied using the CHE model. Formaldehyde and methanol are the competing intermediates and products with methane. Formaldehyde has already been confirmed as the intermediate for the CH_4 formation in our prior experiments. The formation of methanol is more favorable than the formation of CH_4 from our calculations at low potential, due to the weak bonding of atomic oxygen to the [CoP]. However, at more negative potential, methane is the thermodynamically preferred. The electrochemical reduction of methanol conducted by combining CV and OLEMS indeed shows the formation of CH_4 from methanol.

In conclusion, DFT calculations suggest a relatively consistent mechanism for the electrochemical reduction of CO_2 with good agreement between theory and experiment. These new insights offer opportunities to design new catalysts for the CO_2 electrochemical reduction.

3.5. Acknowledgements

J.S. acknowledges the award of a grant of the Chinese Scholarship Council (CSC). This work was supported by the TOP grant from the Netherlands Organization for Scientific Research (NWO). This work is part of the programme 'CO_2 neutral fuels' of the Foundation for Fundamental Research on Matter (FOM), which is financially supported by NWO, co-financed by Shell Global Solutions International B.V..

REFERENCES

1. Hori, Y.; Kikuchi, K.; Suzuki, S., Production of CO and CH_4 in Electrochemical Reduction of CO_2 at Metal Electrodes in Aqeous Hydrogencarbonate Solution. *Chem. Lett.* **1985**, *14*, 1695-1698.

2. Hori, Y.; Murata, A.; Takahashi, R., Formation of Hydrocarbons in the Electrochemical Reduction of Carbon Dioxide at a Copper Electrode in Aqueous Solution. *J. Chem. Soc. Faraday Trans.* **1989**, *85*, 2309-2326.

3. Fisher, B. J.; Eisenberg, R., Electrocatalytic Reduction of Carbon Dioxide by Using Macrocycles of Nickel and Cobalt. *J. Am. Chem. Soc.* **1980**, *102*, 7361-7363.

4. Kortlever, R.; Balemans, C.; Kwon, Y.; Koper, M. T. M., Electrochemical CO2 Reduction to Formic Acid on a Pd-Based Formic Acid Oxidation Catalyst. *Catal. Today* **2015**, *244*, 58-62.

5. Koper, M. T. M., Thermodynamic Theory of Multi-Electron Transfer Reactions: Implications for Electrocatalysis. *J. Electroanal. Chem.* **2011**, *660*, 254-260.

6. Hori, Y. Electrochemical CO_2 Redcution on Metal Electrodes, *Modern Aspects of Electrochemistry*. **2008**.

7. Peterson, A. A.; Abild-Pedersen, F.; Studt, F.; Rossmeisl, J.; Norskov, J. K., How Copper Catalyzes the Electroreduction of Carbon Dioxide into Hydrocarbon Fuels. *Energ. Environ. Sci.* **2010**, *3*, 1311-1315.

8. Schouten, K. J. P.; Kwon, Y.; van der Ham, C. J. M.; Qin, Z.; Koper, M. T. M., A New Mechanism for the Selectivity to C1 and C2 Species in the Electrochemical Reduction of Carbon Dioxide on Copper Electrodes. *Chem. Sci.* **2011**, *2*, 1902-1909.

9. Kortlever R.; Shen J.; Schouten K. J. P.; Calle-Vallejo F.; Koper M. T. M., Catalysts and Reaction Pathways for the Electrochemical Reduction of Carbon Dioxide. *J. Phys. Chem. Lett.* **2015**, 6, 4073-4082.

10. Beley, M.; Collin, J. P.; Ruppert, R.; Sauvage, J. P., Electrocatalytic Reduction of Carbon Dioxide by Nickel $Cyclam^{2+}$ in Water: Study of the Factors Affecting the Efficiency and the Selectivity of the Process. *J. Am. Chem. Soc.* **1986**, *108*, 7461-7467.

11. Yoshida, T.; Kamato, K.; Tsukamoto, M.; Iida, T.; Schlettwein, D.; Wöhrle, D.; Kaneko, M., Selective Electroacatalysis for CO_2 Reduction in the Aqueous Phase Using Cobalt Phthalocyanine/Poly-4-Vinylpyridine Modified Electrodes. *J. Electroanal. Chem.* **1995**, *385*, 209-225.

12. Sonoyama, N.; Kirii, M.; Sakata, T., Electrochemical Reduction of CO_2 at Metal-Porphyrin Supported Gas Diffusion Electrodes under High Pressure CO_2. *Electrochem. Commun.* **1999**, *1*, 213-216.

13. Tripkovic, V.; Vanin, M.; Karamad, M.; Björketun, M. E.; Jacobsen, K. W.; Thygesen, K. S.; Rossmeisl, J., Electrochemical CO_2 and CO Reduction on Metal-Functionalized Porphyrin-Like Graphene. *J. Phys. Chem. C* **2013**, *117*, 9187-9195.

14. Leung, K.; Nielsen, I. M. B.; Sai, N.; Medforth, C.; Shelnutt, J. A., Cobalt–Porphyrin Catalyzed Electrochemical Reduction of Carbon Dioxide in Water. 2. Mechanism from First Principles. *J. Phys. Chem. A,* **2010**, *114*, 10174-10184.

15. Nielsen, I. M. B.; Leung, K., Cobalt–Porphyrin Catalyzed Electrochemical Reduction of Carbon Dioxide in Water. 1. A Density Functional Study of Intermediates. *J. Phys. Chem. A,* **2010**, *114*, 10166-10173.

16. Shen J.; Kortlever R.; Kas R.; Birdja Y. Y.; Diaz-Morales O.; Kwon Y.; Ledezma-Yanez I.; Schouten K. J. P.; Mul G.; Koper M. T.M., Electrocatalytic Reduction of Carbon Dioxide to Carbon Monoxide and Methane at an Immobilized Cobalt Protoporphyrin in Aqueous Solution. *Nat. Commun.* **2015**, 6, article number:8177.

17. te Velde, G.; Bickelhaupt, F. M.; Baerends, E. J.; Fonseca Guerra, C.; van Gisbergen, S. J. A.; Snijders, J. G.; Ziegler, T., Chemistry with Adf. *J. Comput. Chem.* **2001**, *22*, 931-967.

18. Hammer, B.; Hansen, L. B.; Nørskov, J. K., Improved Adsorption Energetics within Density-Functional Theory Using Revised Perdew-Burke-Ernzerhof Functionals. *Phys.Review B* **1999**, *59*, 7413-7421.

19. Grimme, S.; Antony, J.; Ehrlich, S.; Krieg, H., A Consistent and Accurate Ab Initio Parametrization of Density Functional Dispersion Correction (Dft-D) for the 94 Elements H-Pu. *J. Chem. Phys.* **2010**, *132*, 154104.

20. Van Lenthe, E.; Baerends, E. J., Optimized Slater-Type Basis Sets for the Elements 1–118. *J. Comput. Chem.* **2003**, *24*, 1142-1156.

21. Klamt, A.; Schuurmann, G., Cosmo: A New Approach to Dielectric Screening in Solvents with Explicit Expressions for the Screening Energy and Its Gradient. *J. Chem. Soc. Perkin Trans. 2* **1993**, 799-805.

22. Klamt, A., Conductor-Like Screening Model for Real Solvents: A New Approach to the Quantitative Calculation of Solvation Phenomena. *J. Phys. Chem.* **1995**, *99*, 2224-2235.

23. Klamt, A.; Jonas, V., Treatment of the Outlying Charge in Continuum Solvation Models. *J. Chem. Phys.* **1996**, *105*, 9972-9981.

24. Nørskov, J. K.; Rossmeisl, J.; Logadottir, A.; Lindqvist, L.; Kitchin, J. R.; Bligaard, T.; Jónsson, H., Origin of the Overpotential for Oxygen Reduction at a Fuel-Cell Cathode. *J. Phys. Chem. B* **2004**, *108*, 17886-17892.

25. de Groot, M. T.; Koper, M. T. M., Redox Transitions of Chromium, Manganese, Iron, Cobalt and Nickel Protoporphyrins in Aqueous Solution. *Phys. Chem. Chem. Phys.* **2008**, *10*, 1023-1031.

26. Meshitsuka, S.; Ichikawa, M.; Tamaru, K., Electrocatalysis by Metal Phthalocyanines in the Reduction of Carbon Dioxide. *Chem. Commun.* **1974**, 158-159.